

New Journal of Physics

The open-access journal for physics

[Athens/Institutional login](#)

IOP login: Passw

[Create account](#) | [Alerts](#) | [Conta](#)

[IOP Journals Home](#) [IOP Journals List](#) [EJs Extra](#) [This Journal](#) [Search](#) [Authors](#) [Referees](#) [Librarians](#) [User Options](#)

[This volume](#) [▲](#) | [This month](#) [▲](#) | [Abstract](#) [▲](#) | [Content finder](#) [▼](#)

New J. Phys. **11** (2009) 013013

doi:10.1088/1367-2630/11/1/013013

Reversible loss of superfluidity of a Bose–Einstein condensate in a 1D optical lattice

R E Sapiro¹, R Zhang and G Raithel

FOCUS Center and Department of Physics, University of Michigan, Ann Arbor, MI 48109, USA

¹ Author to whom any correspondence should be addressed.

E-mail: resapiro@umich.edu

Received 18 August 2008

Published 7 January 2009

Abstract. We apply a one-dimensional (1D) optical lattice, formed by two laser beams with a wavelength of 852 nm, to a 3D ⁸⁷Rb Bose–Einstein condensate (BEC) in a shallow magnetic trap. We use Kapitza–Dirac scattering to determine the depth of the optical lattice. A qualitative change in behavior of the BEC is observed at a lattice depth of $30E_{\text{rec}}$, where the quantum gas undergoes a reversible transition from a superfluid state to a state that lacks well-to-well phase coherence. Our observations are consistent with a 1D Mott insulator transition, but could also be explained by mean-field effects.

Contents

- [1. Introduction](#)
- [2. Experimental setup and lattice calibration](#)
- [3. Experimental observations](#)
- [4. Discussion](#)
- [5. Conclusion](#)
- [Acknowledgments](#)
- [References](#)

1. Introduction

Bose–Einstein condensation (BEC) was first demonstrated in 1995, creating an explosion of interest in previously unattainable many-body quantum phenomena [1]. Of particular interest is the phase transition from superfluid to Mott insulator [2]. In the three-dimensional (3D) case, this phase transition occurs when a 3D optical lattice is applied to a BEC. As the lattice depth is increased, the BEC transitions from a superfluid state to a state with a definite number of atoms in each lattice well. The Mott insulator transition has drawn the interest of both atomic and condensed matter physicists, due to the possibilities it creates for simulating ideal, controlled condensed matter systems. Under the correct circumstances the transition could be used to create supersolids or other novel phases of matter [3]. Doping the Mott insulator with fermions can be used to simulate a semiconductor [4]. One can use Feshbach resonances to create molecules in a Mott insulator with two atoms per site [5], which could eventually lead to a molecular BEC [6, 7]. The Mott insulator state could also provide a means to entangle neutral atoms and form a quantum register for a quantum

computer (for a review, see [8]). Several laboratories have succeeded in producing the transition from a BEC to a 3D Mott insulator [2, 4, 5, 9]. In lower dimensions, the Mott insulator transition has been achieved using 2D [10, 11] and 1D [12] Bose gases. Attaining the Mott insulator transition requires a deep lattice, commonly achieved by high laser power and narrowly focused beams. Demonstrating the transition from a BEC to a 1D Mott insulator (a 3D BEC in a 1D lattice formed by two laser beams) is more difficult because a deeper lattice is needed [13, 14]. Furthermore, characterizing the transition requires an accurate determination of the lattice depth, which may be complicated due to uncertainties in the lattice beam alignment. In this paper, we experimentally investigate the reversible loss of superfluidity of a 3D BEC in a 1D lattice using a robust method to calibrate the lattice depth [15]. In contrast with [12], we use a 3D Bose gas, applying no transverse lattice potential^{Note2}. Our observations are consistent with a transition to a 1D Mott insulator.

2. Experimental setup and lattice calibration

In the experiment, we start with a ^{87}Rb BEC of $5\text{--}8\times 10^4$ atoms in a practically harmonic magnetic trap. Our BEC apparatus is described in [16]. In the data presented, we use magnetic-trap frequencies of 80 Hz and 200 Hz in the direction of the optical lattice (in the other two directions, the trap frequencies are 20 Hz and 80 Hz or 40 Hz and 200 Hz, respectively). The optical lattice is formed by a retro-reflected, far-off-resonance laser beam (wavelength 852 nm; power up to 200 mW after passage through an optical fiber, which is employed to improve the beam quality). The beam is focused into a spot with an intensity full-width at half-maximum of 80 μm . The depth of the optical lattice is determined as follows.

When a standing wave is applied to cold atoms for a duration that is sufficiently short that the atoms are stationary while the lattice is applied, the system is in the Kapitza–Dirac scattering regime (analogous to the Raman–Nath regime in optics). The 1D optical lattice adds a potential

$$V(x) = -V_0(1 - \cos(2k_L x)) \quad (1)$$

to the atoms over the time interval Δt that the lattice is on. $2V_0$ is the lattice depth, and k_L is the wavenumber of the lattice beams. Assuming an initial wavefunction $\psi(x, t = 0) = 1$, the wavefunction after the lattice pulse is, neglecting a global phase factor,

$$\begin{aligned} \psi(x, t > 0) &= \exp\left(i\frac{V_0\Delta t \cos(2k_L x)}{\hbar}\right) \\ &= \sum_{n=-\infty}^{\infty} (i)^n J_n\left(\frac{V_0\Delta t}{\hbar}\right) \exp(i2nk_L x). \end{aligned} \quad (2)$$

The expression in the sum shows that the BEC breaks up into components with momenta that are integer multiples of $2\hbar k_L$ and with amplitudes given by Bessel functions [17, 18]. In particular, the order $n = 0$ first vanishes at a time Δt_0 for which $V_0 = 2.4048\hbar/\Delta t_0$. The lattice depth $2V_0$ can thus be found by measuring the time Δt at which the $n = 0$ order first vanishes [15]. For an atomic polarizability α and a single-beam lattice intensity I_1 , the lattice depth is also given by $2V_0 = \alpha I_1/(2c\epsilon_0)$. Using the above equations, the lattice depth can be experimentally calibrated against arbitrary linear functions of I_1 , such as the measured beam power. The strength of this method is that no geometrical measurements of the lattice beam size and position are necessary.

To induce Kapitza–Dirac scattering, the optical lattice is applied to the BEC for a few microseconds. The lattice and the trap are then turned off simultaneously. The BEC is allowed to expand freely for times of flight (TOF) of 16 ms or 12 ms, for the case of the 80 Hz or 200 Hz traps, respectively. After the expansion, we take absorption images, shown in figure 1(a). Since the BEC temperature depends on the trap frequency, different trap frequencies require different TOFs to produce the best image. For each scattering order n , we measure the atom number N_n (N_T is the total atom number). In figure 1(b), we plot N_0/N_T versus Δt and find the lattice duration Δt_0 where this ratio first approaches zero; the corresponding lattice depth is $4.81\hbar/\Delta t_0$. In this way, we can determine the proportionality constant relating the lattice-power reading to the lattice depth. Typically, we find $\Delta t_0 \sim 3 \mu\text{s}$. For example, in figure 1, by fitting the N_0/N_T with

$J_0^2(a\Delta t)$, we find $\Delta t_0 = 3.02 \mu\text{s}$, with a fit error of $\sim 1\%$. This is well within the validity range of the short-pulse approximation underlying the above treatment, as evidenced by the fits in figure 1(b) which match the data well up to $6 \mu\text{s}$. In the measurements presented in this paper, this calibration procedure is repeated frequently to account for small changes in the alignment of the lattice beams. Furthermore, this procedure is used to initially align the lattice with respect to the BEC: better overlap between the lattice and the BEC leads to a smaller Δt_0 .

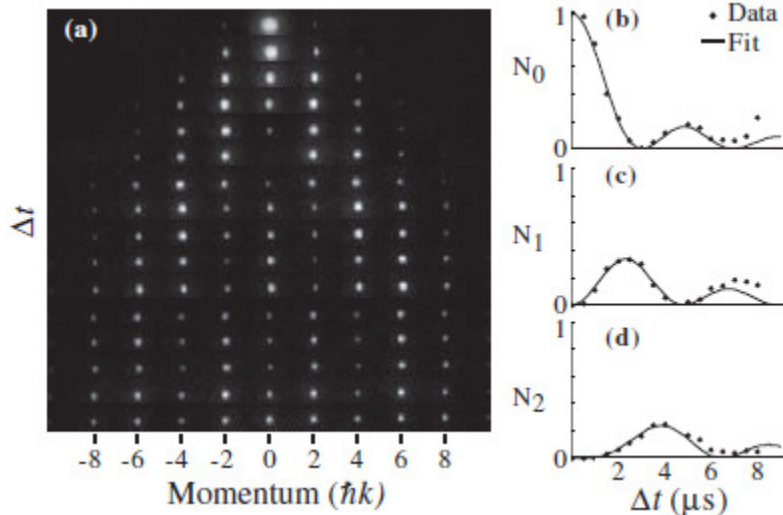


Figure 1. (a) TOF images of Kapitza–Dirac scattering as a function of lattice duration Δt , in steps of $0.5 \mu\text{s}$, starting from $0.5 \mu\text{s}$. (b)–(d) Scattering ratios N_n/N_T , as defined in the text, for the scattering orders $n = 0, 1$ and 2 , respectively, as a function of lattice duration. The data in (b) are fit with $J_0^2(a\Delta t)$, with best-fit parameter $a = 0.79 \mu\text{s}^{-1}$. The lines in (b)–(d) show $J_n^2(0.79 \mu\text{s}^{-1} \Delta t)$ with respective values of n .

Overall, we estimate our lattice depth uncertainty to be $\sim 5\%$. Most of this uncertainty is not intrinsic to the method used for calibration, but rather is due to slow drifts in lattice alignment over the course of our measurements, post-calibration. We typically calibrate our lattice depth once, or occasionally twice, per day, either at the beginning or the end of a data run. The accuracy of the Kapitza–Dirac calibration method compares favorably to estimates of the lattice depth based on measurements of the lattice beam profile, which rely on accurate knowledge of the lattice beam alignment relative to the BEC. If the lattice beam alignment is difficult to determine, as in our case, the beam profile method can lead to huge systematic errors. Finally, we note that there are other lattice depth calibration methods based on parametric heating [19, 20], wave-packet motion [21, 22], and BEC scattering outside the Kapitza–Dirac regime [23]. In principle, all of these methods could yield calibrations of similar precision. However, in our experiment, the calibration method based on Kapitza–Dirac scattering is the easiest to implement.

3. Experimental observations

With the lattice depth calibrated using relatively fast optical lattice pulses, we investigate the loss of well-to-well phase coherence of the BEC when the optical lattice is turned on slowly. We use the amplitude modulation of an acousto-optic modulator to control the power of the lattice beams. We ramp up the power of the lattice beam from zero to its final value over 10 ms, and then hold it there for 5 ms. Then, we simultaneously turn off the lattice and the magnetic trap, and take a TOF measurement. As can be seen in figure 2(b), for small lattice depths the BEC is only slightly modulated by the lattice, corresponding to the appearance of only two weak side peaks, at $\pm 2\hbar k_L$. As the depth of the lattice is increased, well-to-well phase coherence is lost. As a result, the side peaks disappear and the central peak broadens, reflecting the momentum distribution of the localized wavefunction in a single lattice well. We associate the loss of well-to-well phase coherence with a loss of superfluidity. Here, we find that the superfluidity is largely lost for lattices deeper than about $30E_{\text{rec}}$.

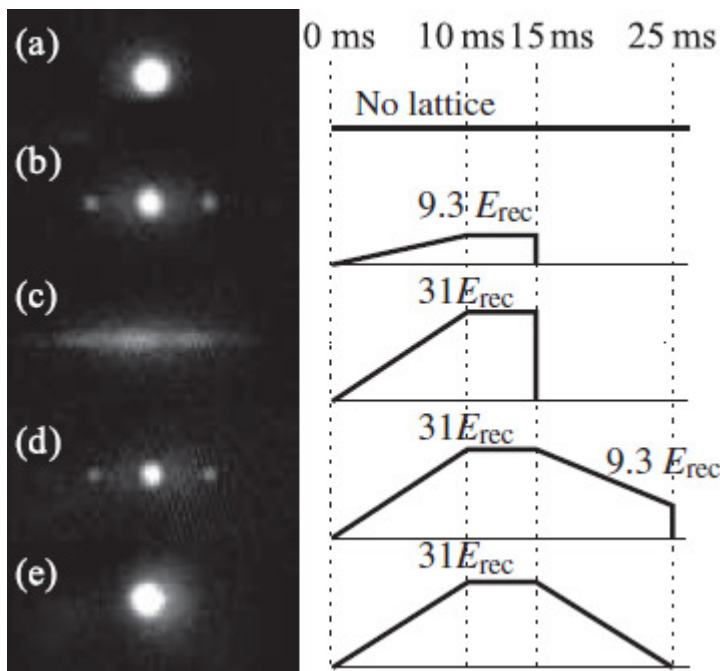


Figure 2. Left: TOF images. Right: lattice depth as a function of time for (a) BEC with no lattice, (b) modulated superfluid in a weak lattice, (c) loss of superfluidity in a deep lattice, (d) modulated superfluidity recovered after the deep lattice is ramped down, and (e) BEC with no lattice, recovered after the deep lattice is ramped down.

The loss of superfluidity in our system is fully reversible. To demonstrate this, we ramp the lattice to $31E_{\text{rec}}$ over 10 ms, hold it there for 5 ms, and then ramp back down over 10 ms. As can be seen in figures 2(d) and (e), we obtain a modulated superfluid and BEC when we ramp down to a weak lattice and no lattice, respectively. The BEC does not appear to have residual momentum components at multiples of $2\hbar k_L$ after the lattice is ramped down.

In lattices deeper than about $30E_{\text{rec}}$, the BEC can be thought of as a stack of phase-uncorrelated pancake BECs. As can be seen in figure 2(c), the atoms expand much farther in the direction of the lattice than in the transverse direction. This is largely due to the momentum spread of the pancake BECs in the lattice-beam direction. Examining the TOF image in figure 2(c), we find a velocity spread of $\Delta p/m_{\text{Rb}} = 8 \text{ mm s}^{-1}$. Using the Heisenberg uncertainty relation, $\Delta x \Delta p \geq \hbar/2$, this corresponds to a localization $\Delta x = 46 \text{ nm}$, or 11% of the lattice period. Neglecting mean-field effects and using the fact that the lattice wells are approximately harmonic near their minima, we find an oscillation frequency of $2\pi \times 35 \text{ kHz}$ for a lattice with a depth of $30E_{\text{rec}}$, and velocity and position uncertainties of 8.9 mm s^{-1} and 41 nm , respectively, for the ground state. These numbers match the values derived from figure 2(c) quite well, showing that the expansion in the lattice-beam direction is mostly driven by the kinetic energy of the pancake BECs in the optical-lattice wells.

A more subtle effect is that in the case of a deep lattice the expansion transverse to the lattice-beam direction is considerably slower than in the lattice-free BEC: about 1.5 and 2.5 mm s^{-1} , respectively. We attribute the difference to a variation in the manifestation of the repulsive mean-field potential (estimated to be $\sim 1 \text{ kHz}$ for our BECs in 200 Hz magnetic traps). Without the lattice, the BEC expansion is driven by a combination of the mean-field pressure and the kinetic energy of the BEC in the magnetic trap, leading to a final expansion speed of about 2.5 mm s^{-1} in all directions in figure 2(a). After application of the deep lattice in figure 2(c), the expansion is mostly driven by the comparatively high kinetic energy of the BEC pancakes in the optical-lattice wells, leading to a much faster expansion in the lattice direction. The faster expansion leads to a reduction of the time over which a substantial mean-field pressure exists, leading to a reduced final expansion speed transverse to the lattice, as observed.

To quantitatively characterize the loss of superfluidity, we examine TOF images as a function of lattice depth. We use the

visibility of the side peaks, v , to map out the transition:

$$v = \frac{N_A - N_B}{N_A + N_B}, \quad (3)$$

where N_A is the linear atom density of one side peak, and N_B is the linear atom density at the minimum between the center peak and the side peak. The timing of the lattice application is as described above. Examining the resulting TOF images, shown in figure 3(a), we take the linear atom density as a function of position in the lattice direction along the central strip of each image, integrating over three pixels in height (a pixel in the image corresponds to $6.7 \mu\text{m}$). For N_A , we choose the local maximum at the side peak, if there is one, and for N_B we choose the local minimum between the side peak and the central peak, as shown in the sample data in figure 3(b). If there is no local side maximum, we designate $v = 0$. We calculate the visibility separately for the side peaks on the left and right, and repeat the calculation for five separate images at each lattice depth. We then average the ten resulting values to get the visibility plotted in figure 3(c). As can be seen, the BEC starts to lose superfluidity around $10E_{\text{rec}}$, where v first reaches a value lower than its initial value. The BEC has fully lost its superfluidity by $30E_{\text{rec}}$, where $v = 0$. The loss of superfluidity happens under the same lattice conditions in the 80 Hz trap and the 200 Hz trap, as can be seen by comparing the circles and triangles in figure 3(c). This indicates that at both 80 Hz and 200 Hz the trap has no noticeable effect compared to the lattice.

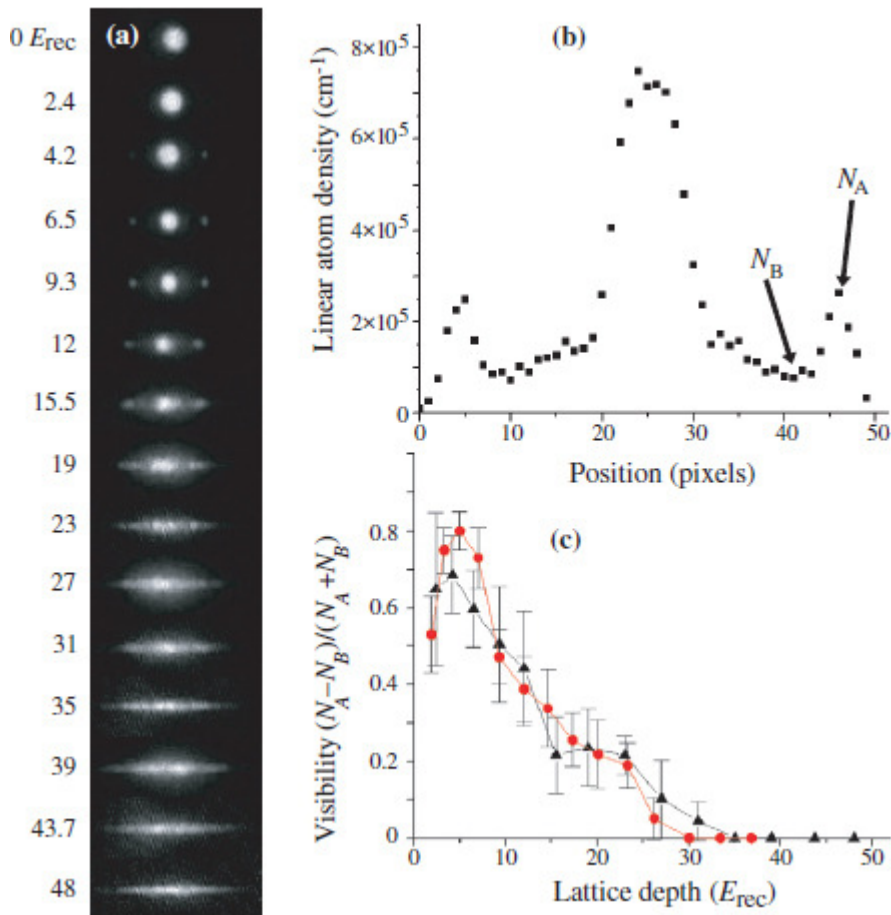


Figure 3. (a) TOF images as a function of lattice depth for a 200 Hz magnetic trap. (b) Linear atom density distribution for a BEC after 12 ms TOF, released from a lattice with a depth of $9.3E_{\text{rec}}$ and magnetic trap with 200 Hz frequency. N_A is the height of the side peak and N_B is the height of the valley. (c) Visibility as a function of lattice depth from a 80 Hz magnetic trap (circles) and a 200 Hz trap (triangles).

Ideally, the visibility should be unity as long as the system is fully in a superfluid state [24]. In the experiment, however, even a minute thermal background will lower the visibility, and will disproportionately affect images with lower N_A . As $N_A, N_B \rightarrow 0$, this will prevent the visibility in equation (3) from reaching unity. For these reasons, the first few data points in figure 3(c) not only fail to approach unity, but are even lower than visibilities seen for lattice depths $\sim 5E_{\text{rec}}$. We are, however, confident that these issues do not affect our determination of where the loss of superfluidity occurs, because the transition happens at a lattice depth where both N_A and N_B are large.

The drop in visibility that is used as an indicator for the reversible loss of well-to-well phase coherence and superfluidity of the BEC (see figure 3) does not always appear instantaneously; it can sometimes take an observable amount of time to develop. To study the dynamics of the dephasing, we ramp the lattice to its final depth over 10 ms, leave the lattice on for a variable hold time, and take TOF images as a function of the hold time, as shown in figure 4(a) for the case of a final depth of $23E_{\text{rec}}$. The visibilities in figure 4(b) are obtained as described earlier. When the lattice is ramped to final depths less than about $10E_{\text{rec}}$, the BEC simply remains superfluid, permanently maintaining a global phase across the individual lattice wells. If the final lattice depth is larger than about $30E_{\text{rec}}$, at the end of the lattice ramp the BEC immediately shows the signatures of a complete loss of superfluidity. Thus, in this case the breakup of the BEC into dephased pancake BECs in the individual lattice wells is already complete by the end of the ramp, and there are no detectable dynamics after completion of the ramp. In contrast, if the BEC is loaded into a moderately deep lattice (of the order of $20E_{\text{rec}}$), it takes a measurable amount of time for the pancake BECs to dephase with respect to each other and for the signatures of the loss of superfluidity to appear. For the parameters in figure 4 it is found that the dephasing takes of the order of 3 ms.

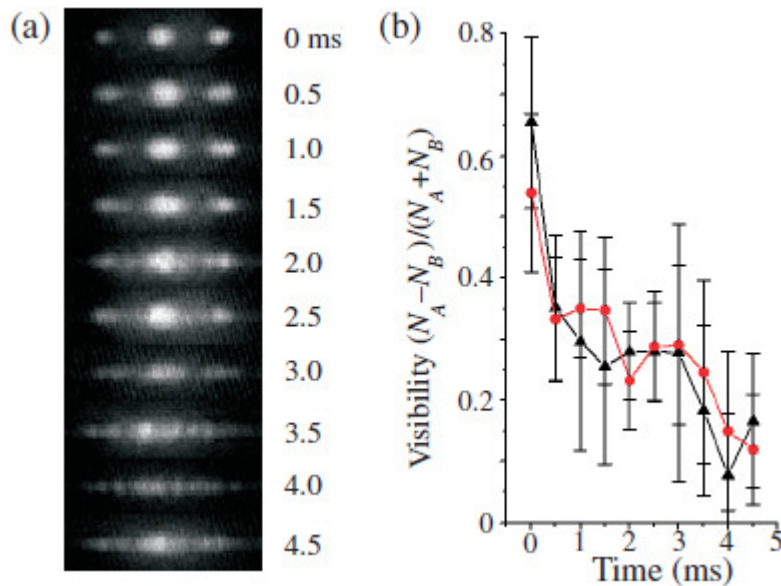


Figure 4. (a) TOF images as a function of holding time in a lattice of $23E_{\text{rec}}$ depth in a 200 Hz magnetic trap. (b) Visibility as a function of holding time of the lattice, for an 80 Hz magnetic trap (circles) and a 200 Hz trap (triangles).

In many of the images where the BEC is in a deep lattice, irregular bright and dark vertical stripes appear. These stripes can be seen in nearly all of the images after the loss of superfluidity from the 80 Hz trap, and several, but not all, of those images from the 200 Hz trap. For example, in figure 3(a), the stripes are visible in the images at 23 and $35E_{\text{rec}}$. The arrangement of the stripes appears random, with no repetition of the pattern from image to image, but the characteristic size of the stripes remains the same for a given magnetic trap frequency. We believe that these stripes represent interference between pancake BECs from different lattice wells during the TOF. After the loss of superfluidity, each pancake BEC still has a definite, but random phase. During the TOF, the pancakes all expand into each other, leading to a characteristic interference speckle size. In figure 5, we show interference patterns in TOF images for the two different magnetic trap depths. To find the characteristic speckle size, Δs , in these images, we take fast Fourier transforms (FFT) of five images and average them for each trap depth. The value of Δs is given by the inverse spatial frequency where the FFT signal reaches the noise floor. We find $\Delta s = 17 \mu\text{m}$ for the 80 Hz trap and $27 \mu\text{m}$ for the 200 Hz trap. Using a

straightforward analysis, we estimate that the number of interfering pancakes, P , is related to Δs and the TOF, T , via $P = 2hT (m \Delta s \lambda)^{-1}$. From this we find $P = 20$ and 10 pancakes for the 80 and 200 Hz traps, respectively. These numbers agree reasonably well with our measurements of the size of the BEC in the respective magnetic traps.



Figure 5. TOF images in a deep lattice and in magnetic traps with frequencies (a) 80 Hz and (b) 200 Hz. The speckles vary from shot to shot, and are due to interference during TOF of pancake BECs from different lattice wells.

4. Discussion

An obvious interpretation of the results presented above is that when the BEC loses its superfluidity it is undergoing a transition into a 1D Mott insulator state. The typical signature of a Mott insulator transition in 3D is that the side peaks disappear and the central peak broadens, reflecting the momentum distribution of the localized wavefunction in a single lattice well [2]. Our system, as seen in figures 2(a)–(c), follows this progression, with an appearance very similar to that of the 3D Mott transition observed in [2, 9]. Furthermore, the Mott insulator transition is a quantum phase transition, and thus is reversible. As seen in figures 2(d) and (e), the loss of superfluidity in our system is also fully reversible. This indicates that the loss of superfluidity is not due to a lattice-induced heating effect, providing support to the Mott insulator explanation of the observed phenomenon.

We observe a complete loss of superfluidity at $30E_{\text{rec}}$. Our system contrasts strongly with that of a 1D Bose gas in a 1D lattice, where the Mott transition is complete around $10E_{\text{rec}}$ [12]. For a 3D Bose gas in a 3D lattice, the Mott transition is complete around $20E_{\text{rec}}$ [2]. Our observations are in general accordance with the prediction in [13] that for a 3D Bose gas in a 1D lattice the Mott transition requires a deeper lattice than in the case of a 3D Bose gas in a 3D lattice. The specifics do not match, however, in that the lattice depth predicted in [13] necessary for the Mott transition is upwards of $50E_{\text{rec}}$ for a system like ours with about 3000 atoms per lattice well.

One concern in the interpretation of our results is adiabaticity. The transition from a superfluid to a Mott insulator should require an adiabatic ramp of the optical lattice, where adiabaticity is related to the timescale of the lattice ramp with respect to the tunneling time of the atoms in the lattice and the energy gap of the insulator. There does not seem to be a strict requirement, however; experiments demonstrating the transition to a 3D Mott insulator have shown that the system only needs to be approximately adiabatic to achieve the transition. In [26], it is observed, for example, that full adiabaticity for a 3D Mott transition requires a ramp time of 100 ms, whereas in [9] it is observed that the Mott transition is achievable for any ramp time larger than 1 ms. Since different lattice depths are required for the 1D Mott transition than for the 3D Mott transition, a direct comparison of times cannot be made. Rather, we compare our experiment to superficially similar experiments done using 1D lattices. Hadzibabic *et al* in [26], performed experiments on a BEC in a 1D optical lattice where they ramp their lattice a factor of approximately 40 times faster than we ramp ours (when measured on a timescale given by the tunneling time); after 10 ms, they have a tunneling time of 7 s, compared to ours of 160 ms. They observe regular interference between the pancake BECs in the different lattice wells. In contrast, we observe random speckle patterns. Furthermore, this random speckle pattern is consistent with the absence of definite phases in a Mott insulating state. Orzel *et al* in [27], meanwhile, found that if the lattice potential is turned on too quickly, the BEC permanently loses superfluidity, even if the lattice potential is slowly ramped back down. We observe a complete return of superfluidity in our system.

McKagan *et al* [28] present an alternate explanation for our results. McKagan *et al* simulate a BEC in a 1D optical lattice using the Gross-Pitaevskii equation. Thus, their analysis does not consider number-squeezing, which is a necessary part of the description of a Mott insulator. Nonetheless, they find that they can simulate a reversible loss of phase coherence. Their results, which they attribute to meanfield effects and a lack of complete adiabaticity, mimic the expected signatures of a 1D Mott insulator. Interestingly, they observe in their simulations that the deepest lattices should produce TOF results resembling our random speckle pattern.

There is little that can be used to distinguish between the two possible interpretations. Qualitatively, the expected

signatures of the Mott transition and a mean-field effect in a nonadiabatic lattice ramp are the same. McKagan *et al* [28] observe, for the case of the mean-field effect, that the visibility of the side peaks should oscillate as a function of lattice depth, unlike the monotonic decrease to $\nu = 0$ expected for a Mott transition. We do not observe any such oscillations. However, McKagan *et al* [28] suggest that these oscillations might not be observable experimentally; rather, they might manifest as heating. We do observe some slight heating when the lattice is ramped up to $30E_{\text{rec}}$ and back down: the thermal halo around the BEC is larger in figure 2(e), after the lattice ramp, than in figure 2(a), before it. McKagan *et al* further hypothesize that the presence of number squeezing (insufficient for a true Mott transition) could damp the oscillations. Thus, the observed lack of oscillations in the visibility function does not allow us to distinguish between a Mott transition and a mean-field effect in a non-adiabatic lattice ramp.

5. Conclusion

In conclusion, we have investigated the reversible loss of superfluidity of a BEC when a deep 1D optical lattice is applied. We used Kapitza–Dirac scattering as an accurate way to calibrate our lattice depth. We examined TOF images of the BEC as a function of lattice depth, and found that the BEC fully loses its superfluidity at about $30E_{\text{rec}}$, and may require a certain time to dephase. Furthermore, we observe random interference patterns in TOF images. Our results are consistent with at least two explanations: most prominently a phase transition from a BEC to a 1D Mott insulator, but also a meanfield effect in a deep lattice. Further research will be required to resolve this ambiguity.

Acknowledgments

We acknowledge the support of the AFOSR grant FA9550-07-1-0412 and the FOCUS (NSF grant PHY-0114336), as well as helpful discussions with Professor Luming Duan.

References

- [1] Anglin J R and Ketterle W 2002 *Nature* **416** 211
[CrossRef Link](#) | [PubMed Abstract](#) | [Order from Infotrieve](#)
- [2] Greiner M, Mandel O, Esslinger T, Hansch T W and Bloch I 2002 *Nature* **415** 39
[CrossRef Link](#) | [PubMed Abstract](#) | [Order from Infotrieve](#)
- [3] Goral K, Santos L and Lewenstein M 2002 *Phys. Rev. Lett.* **88** 170406
[CrossRef Link](#) | [PubMed Abstract](#) | [Order from Infotrieve](#)
- [4] Ospelkaus S, Ospelkaus C, Wille O, Succo M, Ernst P, Sengstock K and Bongs K 2006 *Phys. Rev. Lett.* **96** 180403
[CrossRef Link](#) | [PubMed Abstract](#) | [Order from Infotrieve](#)
- [5] Rom T, Best T, Mandel O, Widera A, Greiner M, Hansch T W and Bloch I 2004 *Phys. Rev. Lett.* **93** 073002
[CrossRef Link](#) | [PubMed Abstract](#) | [Order from Infotrieve](#)
- [6] Jaksch D, Venturi V, Cirac J L, Williams C J and Zoller P 2002 *Phys. Rev. Lett.* **89** 040402
[CrossRef Link](#) | [PubMed Abstract](#) | [Order from Infotrieve](#)
- [7] Moore M G and Sadeghpour H R 2003 *Phys. Rev. A* **67** 041603
[CrossRef Link](#) | [Order from Infotrieve](#)
- [8] Jaksch D 2004 *Contemp. Phys.* **45** 367–81
[CrossRef Link](#) | [Order from Infotrieve](#)
- [9] Xu K, Liu Y, Abo-Shaer J R, Mukaiyama T, Chin J K, Miller D E, Ketterle W, Jones K M and Tiesinga E 2005 *Phys. Rev. A* **72** 043604
[CrossRef Link](#) | [Order from Infotrieve](#)
- [10] Spielman I B, Phillips W D and Porto J V 2007 *Phys. Rev. Lett.* **98** 080404
[CrossRef Link](#) | [PubMed Abstract](#) | [Order from Infotrieve](#)
- [11] Kohl M, Moritz H, Stoferle T, Schori C and Esslinger T 2005 *J. Low Temp. Phys.* **138** 635
[CrossRef Link](#) | [Order from Infotrieve](#)
- [12] Stoferle T, Moritz H, Schori C, Kohl M and Esslinger T 2004 *Phys. Rev. Lett.* **92** 130403
[CrossRef Link](#) | [PubMed Abstract](#) | [Order from Infotrieve](#)
- [13] Li J, Yu Y, Dudarev A M and Niu Q 2006 *New J. Phys.* **8** 154
[IOP Article](#)
- [14] van Oosten D, van der Straten P and Stoof H T C 2003 *Phys. Rev. A* **67** 033606
[CrossRef Link](#) | [Order from Infotrieve](#)
- [15] Behinaein G, Ramareddy V, Ahmadi P and Summy G S 2006 *Phys. Rev. Lett.* **97** 244101
[CrossRef Link](#) | [PubMed Abstract](#) | [Order from Infotrieve](#)

- [16] Zhang R, Sapiro R E, Morrow N V, Mhaskar R R and Raithel G 2008 *Phys. Rev. A* **77** 063615
[CrossRef Link](#) | [Order from Infotrieve](#)
- [17] Bartell L S, Roskos R R and Thompson H B 1968 *Phys. Rev.* **166** 1494
[CrossRef Link](#) | [Order from Infotrieve](#)
- [18] Gould P L, Ruff G A and Pritchard D E 1986 *Phys. Rev. Lett.* **56** 827
[CrossRef Link](#) | [PubMed Abstract](#) | [Order from Infotrieve](#)
- [19] Friebe S, D'Andrea C, Walz J, Weitz M and Hänsch T W 1998 *Phys. Rev. A* **57** R20
[CrossRef Link](#) | [Order from Infotrieve](#)
- [20] Wu J, Newell R, Hausmann M, Vieira D J and Zhao X 2006 *J. Appl. Phys.* **100** 054903
[CrossRef Link](#) | [Order from Infotrieve](#)
- [21] Raithel G, Birkel G, Phillips W D and Rolston S L 1997 *Phys. Rev. Lett.* **78** 2928
[CrossRef Link](#) | [Order from Infotrieve](#)
- [22] Rudy P, Eijnisman R and Bigelow N P 1997 *Phys. Rev. Lett.* **78** 4906
[CrossRef Link](#) | [Order from Infotrieve](#)
- [23] Ovchinnikov Yu B, Müller J H, Doery M R, Vredendregt E J D, Helmerson K, Rolston S L and Phillips W D 1999 *Phys. Rev. Lett.* **83** 284
[CrossRef Link](#) | [Order from Infotrieve](#)
- [24] Diener R B, Zhou Q, Zhai H and Ho T-L 2007 *Phys. Rev. Lett.* **98** 180404
[CrossRef Link](#) | [PubMed Abstract](#) | [Order from Infotrieve](#)
- [25] Gericke T, Gerbier F, Widera A, Fölling S, Mandel O and Bloch I 2007 *J. Mod. Opt.* **54** 735
[CrossRef Link](#) | [Order from Infotrieve](#)
- [26] Hadzibabic Z, Stock S, Battelier B, Bretin V and Dalibard J 2004 *Phys. Rev. Lett.* **93** 180403
[CrossRef Link](#) | [PubMed Abstract](#) | [Order from Infotrieve](#)
- [27] Orzel C, Tuchman A K, Fenselau M L, Yasuda M and Kasevich M A *Science* **291** 2386
[PubMed Abstract](#)
- [28] McKagan S B, Feder P L and Reinhardt W P 2006 *Phys. Rev. A* **74** 013612
[CrossRef Link](#) | [Order from Infotrieve](#)

Notes

Note2 In our work, the parameter V_{\square} used in [12] is $V_{\square} = 0$.

[This volume](#) ▲ | [This month](#) ▲ | [Abstract](#) ▲

CONTENT FINDER New Journal of Physics

Full Search
 Help

Author: | Vol/Year: | Issue/Month: | Page/Article No: | Find

[IOP Journals Home](#) | [IOP Journals List](#) | [EJs Extra](#) | [This Journal](#) | [Search](#) | [Authors](#) | [Referees](#) | [Librarians](#) | [User Options](#) | [Help](#) | [Recommend this journal](#)
 Copyright © 1998-2009 Deutsche Physikalische Gesellschaft & Institute of Physics

